Publication title	**Large eddy simulation of the Delft Adelaide Flame III using a quadrature-based method of moments**
Authors	F. Ferraro, S. Gierth, S. Salenbauch, W. Han, C. Hasse
Issue Date	April 2021
Publisher	European Combustion Meeting 2021
Type of publication	Conference proceeding
Acknowledgement	The ESTiMatE project has received funding from the Clean Sky 2 Joint Undertaking under the European Union's Horizon 2020 research and innovation programme under grant agreement No 821418.
Disclaimer	

Large eddy simulation of the Delft Adelaide Flame III using a quadrature-based method of moments

F. Ferraro[*,1], S. Gierth[1], S. Salenbauch[1], W. Han[1,2], C. Hasse[1]

[1]Institute for Simulation of Reactive Thermo-Fluid Systems (STFS), Technische Universität Darmstadt, Otto-Berndt-Straße 2, Darmstadt 64287, Germany

[2]School of Engineering, University of Edinburgh, Edinburgh EH8 3JL, Scotland, UK

Abstract

In this work, the recently developed split-based Extended Quadrate Method of Moments (S-EQMOM) is combined with a LES/presumed PDF-based flamelet/progress variable approach to achieve the predictions of soot particle size distributions in a turbulent non-premixed jet flame. The advantage of the S-EQMOM is that a continuous soot particle number density function (NDF) is able to be reconstructed by superimposing kernel density functions (KDFs) of presumed shape (gamma or log-normal distribution) that interact through the particle coagulation. Moreover, the S-EQMOM primary nodes are determined individually for each KDF yielding improvement in the numerical robustness compared to classical EQMOM. The above numerical framework is employed to predict soot particle formation in the Delft Adelaide flame III, which is a benchmark flame of the International Sooting Flame (ISF) workshop. The target flame is featured by low/high sooting propensity/intermittency and by relatively comprehensive flow/scalar/soot data available for validating the model framework. Simulation results are compared with the experimental results and discussed for both the gas phase and the particulate phase. A satisfactory quantitative agreement has been obtained especially in terms of soot volume fraction. The ability of the S-EQMOM to provide information on particle size distribution indicates a dominant unimodal distribution along the flame centerline.

Introduction

Carbon particulate produced by the combustion of hydrocarbon fuels is not only one of the major causes of global warming and accelerated ice melting, but also an increased risk for human health due to particle inhalation. Accurate predictions of particle number concentration as well as size distribution are necessary to meet stringent pollutant regulations and develop potential ways to reduce the health effects of particulate matter. However, modeling soot particle formation and growth pathways in turbulent reacting flows still represents a challenge due to the complex multiscale interaction between turbulence, chemical reactions, and particle evolution that is characterized by a particle number density function (NDF). Sectional methods (SMs) [1]–[4] and method of moments (MOM) [5]–[8] are the most widely used approaches to determine the soot NDF in turbulent reacting flows.

SMs are based on the discretization of the internal coordinates of the NDF resulting in a set of transport equations for the soot evolution and provide local information of particle size distribution (PSD).

On the other hand, the MOM does not discretize the NDF directly but provides a good approximation of the NDF by solving transport equations for the low-orders moments of the NDF, in combination with an appropriate reconstruction method. This results in a computationally efficient strategy to evaluate soot population, suitable to be combined with reacting LES. However, the transformation of the PBE to moment transport equations leads to unclosed terms, which for soot application have been closed with different approaches as MOMIC, HMOM [5], [6], [9], or quadrature-based method of moments (QMOM) [10]–[14]. Among the different QMOM, the extended QMOM (EQMOM) approach [10] has shown to be suitable for soot prediction, since it provides a continuous reconstruction of the NDF, particularly important when soot particle oxidation needs to be considered. However, the EQMOM algorithm has shown some numerical issues that make the approach difficult to be integrated in complex three-dimensional reacting simulations.

Recently, following the idea of Megaridis and Dobbins [15] to consider the NDF as a sum of KDFs interacting via the coagulation term, Salenbauch et al. [16] have formulated an alternative extended QMOM, the so-called split-based Extended QMOM approach (S-EQMOM), to overcome the numerical difficulties of the EQMOM. The S-EQMOM yields a continuous NDF by superimposing kernel density functions (KDF), similarly to the EQMOM, but solving transport equations for the lower moments of each coupled KDF (or sub-NDF as in [16]).

Therefore, the S-EQMOM provides a numerically robust algorithm to reconstruct the soot particle NDF. The validity of the method has been demonstrated by simulating laminar premixed flames with uni- and bi-modal soot particle distribution and a two-stage burner flame configuration with significant soot oxidation [17]. Nevertheless, the performance of S-EQMOM in modeling soot formation in turbulent flames has not been examined. With this background, the focus of this work is to integrate the S-EQMOM method in the LES context for simulations of turbulent sooting flames and investigations of the soot particle evolution and size distribution. The numerical framework is validated by simulating the Delft Adelaide Flame III that is one of the

[*] Corresponding author: ferraro@stfs.tu-darmstadt.de (F. Ferraro)

Proceedings of the European Combustion Meeting 2021

target flames of the 'International Sooting Flame Workshop' (ISF) [18], [19].
In the following, the numerical modeling is presented first. The flow field and soot properties are discussed and compared with the experimental data [18], [19]. Finally, the particle number density function is reconstructed and analyzed.

Numerical Modeling

Soot Modeling

The evolution of the soot particle number density function (NDF) is governed by the population balance equation (PBE) [16], [20]. The NDF $n(t, \boldsymbol{x}; \boldsymbol{\xi})$ depends on time t, space $\boldsymbol{x}$, and internal coordinate $\boldsymbol{\xi}$. In this study, soot particles are considered spherical. Thus, the vector of the internal coordinates $\boldsymbol{\xi}$ is defined as $\boldsymbol{\xi} = [V]$, leading to a univariate model formulation.
The S-EQMOM method, recently developed in [16] is used. In the S-EQMOM the moments $m_k^{s_\alpha}$ of N_s sub-NDFs $n_{s_\alpha}(V)$ are considered instead of the moment of the entire NDF, $n(V)$, as in standard EQMOM [10], [13]. A generic sub-NDF moment is defined as

$$m_k^{s_\alpha} = \int_{V_{\min}}^{\infty} V^k n_{s_\alpha}(V) dV \tag{1}$$

where s_α is the index of the sub-NDF. The entire NDF may then be approximated as

$$n(\tilde{V}) = \sum_{\alpha=1}^{N_{sub}} n_{s_\alpha}(\tilde{V}) \approx \sum_{\alpha=1}^{N_{sub}} w_{s_\alpha} \delta_{\sigma_{s_\alpha}} \left(\tilde{V}; \tilde{V}_{s_\alpha}\right) \tag{2}$$

In S-EQMOM the moment inversion procedure consists in the analytical evaluation of the nodes' positions V_{s_α}, their weights w_{s_α} and the scale parameters σ_{s_α} directly from the first three moments $\left[m_0^{s_\alpha}, m_1^{s_\alpha}, m_2^{s_\alpha}\right]^T$ of the N_s sub-NDFs. Note that this corresponds to the inversion of a series of one-node EQMOM systems using the solution algorithm proposed in [10].
The main advantage of the S-EQMOM over the EQMOM is that the inversion procedure produces a system of equations which is solved analytically and has a unique solution [16], while the inversion in the EQMOM is an iterative and non-unique procedure [10], [21], [22] applied to a set of low and high order moments of the entire NDF. This greatly improves the stability of the inversion algorithm, allowing a computationally efficient and robust reconstruction of the soot particle NDF.
The source terms of the moment equations include particle nucleation from dimerization of two PAH molecules, surface growth by condensation of PAH molecules on soot particles and H-abstraction-C_2H_2-addition (HACA) mechanism, coagulation and particle oxidation by reactions with O_2 and OH.
Further details regarding the S-EQMOM formulation and the moment source terms definition can be found in [16].

Combustion Modeling

In the present study, the FPV framework [23], [24] based on steady laminar diffusion flames manifold is employed. The flamelet solutions are generated by solving the steady-state flamelet equations [25] with different stoichiometric scalar dissipation rates ranging from thermochemical equilibrium to quenching conditions. The kinetic mechanism presented in [26], [27] is utilized here. The thermochemical state is parametrized by the mixture fraction Z, the scalar dissipation rate χ_{st}, which is mapped to the progress variable defined as $Y_C = Y_{H_2O} + Y_{H_2} + Y_{CO_2} + Y_{CO}$ in this study. Note, that radiation effects are neglected here.

Coupled LES-FPV approach

The flow field is described by the Favre-filtered Navier-Stokes equations. The turbulence closure is achieved using the eddy viscosity hypothesis employing the σ-model [28], with model constant dynamically determined with the procedure described in [29]. The suitability of this LES-FPV coupling for turbulent jet flames was previously shown in [30]–[32]. The Favre-filtered transport equation of mixture fraction and progress variable are

$$\frac{\partial}{\partial t}(\bar{\rho}\tilde{Z}) + \nabla \cdot (\bar{\rho}\tilde{\boldsymbol{u}}\tilde{Z}) = \nabla \cdot \left[\bar{\rho}\left(D_Z + \frac{\nu_t}{\mathrm{Sc_t}}\right)\nabla\tilde{Z}\right] \tag{3}$$

$$\frac{\partial}{\partial t}\left(\bar{\rho}\widetilde{Y_C}\right) + \nabla \cdot \left(\bar{\rho}\tilde{\boldsymbol{u}}\widetilde{Y_C}\right) = \nabla \cdot \left[\bar{\rho}\left(D_{Y_C} + \frac{\nu_t}{\mathrm{Sc_t}}\right)\nabla\widetilde{Y_C}\right] + \bar{\dot{\omega}}_{Y_C} \tag{4}$$

Here, D_Z and D_{Y_C} denote the diffusion coefficient of the mixture fraction and progress variable, respectively, which are evaluated under the assumption of unity Lewis number as $D_Z \equiv D_{Y_C} = \alpha$, with the thermal diffusivity α determined from the flamelet table. Furthermore, υ_t represents the eddy viscosity, the turbulent Schmidt number Sc_t is set to 0.7, and $\bar{\dot{\omega}}_{Y_C}$ is the filtered source term of the transported variable, which is also obtained from the look-up table. The variance of the mixture fraction is calculated using an algebraic equation following [23].

The thermo-chemical state is retrieved using a normalized progress variable $\tilde{C}$ [33] defined as

$$\tilde{C} = \frac{\tilde{Y}_C - \tilde{Y}_{C,\min}(\tilde{Z})}{\tilde{Y}_{C,\max}(\tilde{Z}) - \tilde{Y}_{C,\min}(\tilde{Z})} \tag{5}$$

Here, the minimum and maximum progress variable values are functions of the mixture fraction and are determined from the tabulated flamelet solutions. The manifold is parametrized as $\tilde{\phi} = \left(\tilde{Z}, \widetilde{Z''^2}, \tilde{C}\right)$. To account for non-resolved fluctuations, a presumed β-shaped filtered density function (FDF) is used for the mixture fraction, whereas a δ-FDF is applied for the progress variable.

To model the slow PAH chemistry and the mass transfer from gas to solid phase due to nucleation of soot particles, a filtered transport equation for the PAH mass fraction is solved following [6]

$$\frac{\partial \bar{\rho}\tilde{Y}_{PAH}}{\partial t} + \frac{\partial \bar{\rho}\tilde{u}_i\tilde{Y}_{PAH}}{\partial x_i} = \frac{\partial}{\partial x_i}\left(\bar{\rho}\tilde{u}_i\tilde{Y}_{PAH} - \bar{\rho}\overline{u_i Y}_{PAH}\right) + \frac{\partial}{\partial x_i}\left(\bar{\rho}\tilde{D}\frac{\partial \tilde{Y}_{PAH}}{\partial x_i}\right) + \bar{\dot{\omega}}_{PAH} \quad (6)$$

Here $\tilde{Y}_{PAH}$ is the sum of the PAH soot precursors considered. According to [6], [34] the filtered source term $\overline{\dot{\omega}_{PAH}}$ is decomposed in three components: a chemical production term $\dot{\omega}_{PAH}{}^{+}$, which is independent of the PAH species concentration, a chemical consumption term $\dot{\omega}_{PAH}{}^{-}$, which scales linear with the PAH species concentration, and a consumption term representing the mass transfer rate from gas-phase to soot $\dot{\omega}_{nuc}$, which scales quadratically with the PAH species concentration,

$$\dot{\omega}_{PAH} = \dot{\omega}^{+}_{PAH} + \dot{\omega}^{-}_{PAH} + \dot{\omega}_{nuc}. \quad (7)$$

The filtered source term will be decomposed analogously to [35]

$$\bar{\dot{\omega}}_{PAH} = \bar{\dot{\omega}}^{+T}_{PAH} + \bar{\dot{\omega}}^{-T}_{PAH}\left(\frac{\tilde{Y}_{PAH}}{\tilde{Y}^{T}_{PAH}}\right) + \bar{\dot{\omega}}^{T}_{nuc}\left(\frac{\tilde{Y}_{PAH}}{\tilde{Y}^{T}_{PAH}}\right)^{2} \quad (8)$$

where the superscript T indicates the value obtained from the flamelet table. It is important to note that the rate of soot particle nucleation $\dot{\omega}_{nuc}$ can be determined in the laminar flamelet calculation since it is only dependent on the gas-phase soot precursor concentrations. Therefore, it can be easily obtained along with the thermo-physical state.

Results and Discussion

Experimental and numerical setup

The experimental setup under investigation is the Delft-Adelaide Flame III from the International Sooting Flame workshop. The burner was first described in [18] and consists of a central main fuel jet of 6 mm diameter. It is surrounded by a rim containing 12 pilot flames stabilizing the main flame, a primary air annular coflow with inner and outer diameters equal to 15 mm and 45 mm, respectively, and a secondary coflow. The fuel jet has a bulk velocity of 21.94 m/s, the coflow streams of 4.4 and 0.3 m/s, respectively. The fuel composition is varying between the different experiments performed on this burner. As mentioned by [19], the sensitivity to the temperature is small with respect to the variation in fuel composition. On the other hand, since the evolution of soot precursors depends strongly on the fuel mixture, the Dutch natural gas composition, used to perform the soot measurements, was chosen in the current investigation. Experimental data for the gas-phase are reported by [18], [35], [36] while the soot measurements are available in [19].

The numerical simulations are performed using the foam-extend 4.0 version of OpenFOAM to solve the filtered Navier-Stokes, transported scalar, and moment equations. The in-house QMOM library is coupled to the CFD solver for the determination of the moment source terms and the reconstruction of the soot particle NDF.

The domain is discretized by a block-structured mesh with approximately 11 mio. cells.

Second-order backward discretization scheme is used for the time and a second-order CDS scheme is applied for the velocity. A TVD scheme utilizing the Sweby [37] limiter is used for discretization of the convective scalar flux.

In the S-EQMOM the NDF is described using a gamma distribution for each of $N_s = 2$ sub-NDFs, which is a proper number to approximate typical bimodal soot particle distribution, as shown in [16]. This yields six additional transport equations to solve the first three moments of each sub-NDFs.

For the generation of the turbulent inflow boundary conditions at the main jet and the first coflow, the upstream geometry of the burner is simulated.

Simulation results

In this section, the simulation results of the gas-phase compared to the experimental data from [35], [36] are first introduced. Then, the soot-related quantities compared with the measurements from [19] are presented and discussed.

Figure 1 shows the mean radial profiles for the axial velocity, mixture fraction, temperature and their rms at three axial locations x/D=16.66, 25 and 41.66 close to nozzle, where experimental data for the flow variables are available. It can be observed that the simulation results are in very good with the experimental data at all axial locations.

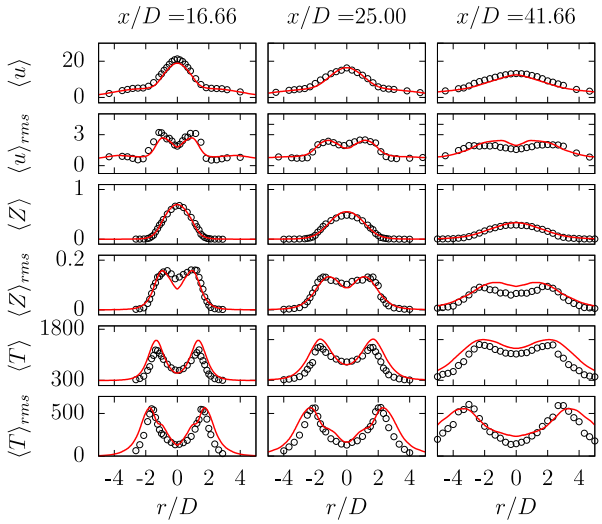

Figure 1 Mean radial profiles of the axial velocity, mixture fraction and temperature and their rms at three axial positions compared with the experimental data [36]. Line: LES; Symbols: Exp. data.

Mean radial profiles of the major species H_2O, CO_2 and minor species, CO and H_2, are shown in Fig. 2. Here, a good comparison is also achieved. At $x/D = 8.3$ CO_2 appears overpredicted. This is due to the slightly different

composition of the natural gas used to perform those experimental measurements and is in line with previous numerical publications [6], [9].

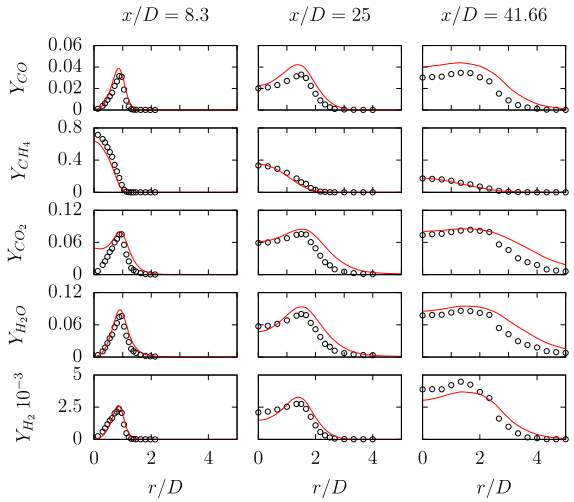

Figure 2 Mean radial profiles of CO, CH_4, H_2O and H_2 mass fraction at three axial positions compared with the experimental data [35]. Line: LES; Symbols: Exp. data.

Mean contours of the temperature, PAH mass fraction, soot volume fraction, and number density are shown in Fig. 3. The superimposed black line represents the stoichiometric mixture fraction isoline ($Z_{st} = 0.073$).

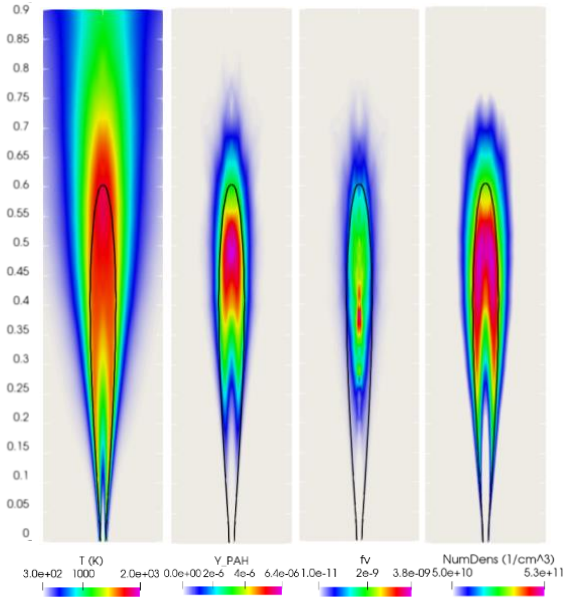

Figure 3 Contour plot of the mean temperature, PAH mass fraction, soot volume fraction and particle number density. The black line represents the stoichiometric mixture fraction.

It can be observed that the soot precursor Y_{PAH} is present in an appreciable amount in the region 0.15 m $< x <$ 0.8 m. A significant soot volume fraction is obtained downstream in the flame for $x >$ 0.3 m. Moreover, the number density contour indicates that the number of particles per LES cell increases due to particle nucleation for $x >$ 0.15 m, while decreases rapidly for $x >$ 0.6 m where coagulation and subsequently particle oxidation ($Z < Z_{st}$) are active. Similarly, particle surface growth (i.e., condensation + HACA) is active for $x >$ 0.15 m, where a large number of particles and PAH molecules are present. In Fig. 4 the mean profile of soot volume fraction along the flame centerline is compared with the experimental data. A quite good agreement can be observed in terms both of peak value and peak position. Soot particles are completely oxidized at $x/D = 120$, upstream the location showed in the experiments. Although the peak value is slightly overpredicted and the peak position is located upstream compared to the experimental data, these results represent a dramatic improvement compared to some recently published results of the same flame [38]–[40]. A comparable agreement is, instead, observed with the results reported by Mueller and Pitsch [6] and by Han et al. [9], based on the hybrid method of moments (HMOM) approach.
Compared to the HMOM approach, S-EQMOM provides a unique advantage that the continuous soot PSD can be directly reconstructed. Figure 5 shows the instantaneous PSD at five axial locations along the centerline. The plots indicate a dominant unimodal distribution. Along the centerline, the number of small particles ($d_p \leq 100$ nm) first increases due to the soot particle nucleation between x/D =30 and x/D =60, where a high amount of PAH molecules is formed. For $x/D > 60$ the particle number decreases due to particle coagulation and then oxidation. It can be observed that at $x/D = 99$ the particle number is significantly reduced with a small diameter due to particle oxidation.

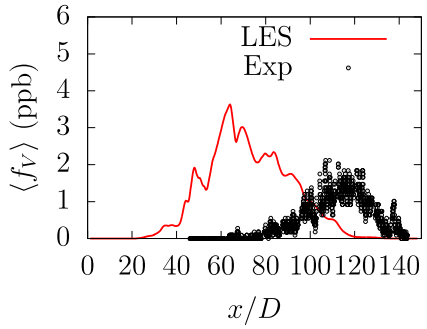

Figure 4 Mean soot volume fraction along the centerline compared with the experimental data [19].

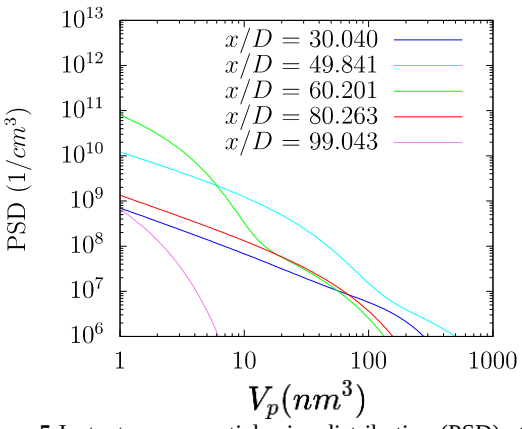

Figure 5 Instantaneous particle size distribution (PSD) at five positions along the centerline.

Conclusions

In this study, a novel split-based EQMOM (S-EQMOM) approach that is capable of reconstructing continuous particle size distributions is coupled with the LES/FPV model, in order to predict soot formation and evolution in the turbulent sooting Delft-Adelaide Flame III. Numerical results of the gas-phase show very good agreement with the experimental measurements available in the lower portion of the flame, close to the nozzle exit. While a monovariate approach is used, the current numerical framework provides a significant improvement in predicting soot volume fraction. It is noted that the S-EQMOM is able to reconstruct instantaneous and continuous particle size distributions (PSD), which is not directly available in the classical method of moments. The investigation of PSD along the centerline shows that a unimodal particle distribution is dominant in this turbulent flame, with particle diameter smaller than 100 nm, which is different from a bimodal distribution commonly observed in laminar flames. Finally, this work demonstrates the good predictive capability of the S-EQMOM both in terms of soot volume fraction and NDF, which is encouraging for the study of carbon-neutral sustainable combustion devices.

Acknowledgements

This research has been funded by the Clean Sky 2 Joint Undertaking under the European Union's Horizon 2020 research and innovation programme under the ESTiMatE project, grant agreement No 821418. Calculations for this research were conducted on the Lichtenberg high-performance computer at TU Darmstadt.

References

[1] D. Grosschmidt, P. Habisreuther, and H. Bockhorn, "Calculation of the size distribution function of soot particles in turbulent diffusion flames," *Proc. Combust. Inst.*, vol. 31 I, no. 1, pp. 657–665, 2007.

[2] K. Netzell, H. Lehtiniemi, and F. Mauss, "Calculating the soot particle size distribution function in turbulent diffusion flames using a sectional method," *Proc. Combust. Inst.*, vol. 31, no. 1, pp. 667–674, Jan. 2007.

[3] P. Rodrigues, B. Franzelli, R. Vicquelin, O. Gicquel, and N. Darabiha, "Coupling an LES approach and a soot sectional model for the study of sooting turbulent non-premixed flames," *Combust. Flame*, vol. 190, pp. 477–499, 2018.

[4] M. Grader, C. Eberle, P. Gerlinger, and M. Aigner, "LES of a pressurized, sooting aero-engine Model Combustor at different equivalence ratios with a sectional approach for PAHs and Soot," in *ASME Turbo Expo 2018: Turbine Technical Conference and Exposition*, 2018, pp. GT2018-75254.

[5] A. Attili, F. Bisetti, M. E. Mueller, and H. Pitsch, "Formation, growth, and transport of soot in a three-dimensional turbulent non-premixed jet flame," *Combust. Flame*, vol. 161, no. 7, pp. 1849–1865, 2014.

[6] M. E. Mueller and H. Pitsch, "LES model for sooting turbulent nonpremixed flames," *Combust. Flame*, vol. 159, no. 6, pp. 2166–2180, 2012.

[7] Y. Xuan and G. Blanquart, "Effects of aromatic chemistry-turbulence interactions on soot formation in a turbulent non-premixed flame," *Proc. Combust. Inst.*, vol. 35, no. 2, pp. 1911–1919, 2015.

[8] H. Koo, M. Hassanaly, V. Raman, M. E. Mueller, and K. P. Geigle, "Large-Eddy Simulation of Soot Formation in a Model Gas Turbine Combustor," *J. Eng. Gas Turbines Power*, vol. 139, no. 3, 2017.

[9] W. Han, V. Raman, M. E. Mueller, and Z. Chen, "Effects of combustion models on soot formation and evolution in turbulent nonpremixed flames," *Proc. Combust. Inst.*, vol. 37, no. 1, pp. 985–992, 2019.

[10] C. Yuan, F. Laurent, and R. O. Fox, "An extended quadrature method of moments for population balance equations," *J. Aerosol Sci.*, vol. 51, pp. 1–23, 2012.

[11] S. Salenbauch, A. Cuoci, A. Frassoldati, C. Saggese, T. Faravelli, and C. Hasse, "Modeling soot formation in premixed flames using an Extended Conditional Quadrature Method of Moments," *Combust. Flame*, vol. 162, no. 6, pp. 2529–2543, Jun. 2015.

[12] S. Salenbauch, M. Sirignano, D. L. Marchisio, M. Pollack, A. D. Anna, and C. Hasse, "Detailed particle nucleation modeling in a sooting ethylene flame using a Conditional Quadrature Method of Moments (CQMOM)," *Proc. Combust. Inst.*, vol. 36, no. 1, pp. 1–9, 2016.

[13] A. Wick, T. Nguyen, F. Laurent, R. O. Fox, and H. Pitsch, "Modeling soot oxidation with the Extended Quadrature Method of Moments," *Proc. Combust. Inst.*, vol. 36, no. 1, pp. 789–797, 2017.

[14] F. Ferraro, C. Russo, R. Schmitz, C. Hasse, and M. Sirignano, "Experimental and numerical study on the effect of oxymethylene ether-3 (OME3) on soot particle formation," *Fuel*, vol. 286, p. 119353, Feb. 2021.

[15] C. M. Megaridis and R. A. Dobbins, "A Bimodal Integral Solution of the Dynamic Equation for an Aerosol Undergoing Simultaneous Particle Inception and Coagulation," *Aerosol Sci. Technol.*, vol. 12, no. 2, pp. 240–255, Jan. 1990.

[16] S. Salenbauch, C. Hasse, M. Vanni, and D. L. Marchisio, "A numerically robust method of moments with number density function reconstruction and its application to soot formation, growth and oxidation," *J. Aerosol Sci.*, vol. 128, pp. 34–49, 2019.

[17] C. A. Echavarria, I. C. Jaramillo, A. F. Sarofim, and J. S. Lighty, "Studies of soot oxidation and

fragmentation in a two-stage burner under fuel-lean and fuel-rich conditions," vol. 33, pp. 659–666, 2011.

[18] T. W. J. Peeters, P. P. J. Stroomer, J. E. de Vries, D. J. E. M. Roekaerts, and C. J. Hoogendoorn, "Comparative experimental and numerical investigation of a piloted turbulent natural-gas diffusion flame," *Symp. Combust.*, vol. 25, no. 1, pp. 1241–1248, 1994.

[19] N. H. Qamar, Z. T. Alwahabi, Q. N. Chan, G. J. Nathan, D. Roekaerts, and K. D. King, "Soot volume fraction in a piloted turbulent jet non-premixed flame of natural gas," *Combust. Flame*, vol. 156, no. 7, pp. 1339–1347, 2009.

[20] D. L. Marchisio and R. O. Fox, *Computational Models for Polydisperse Particulate and Multiphase Systems*. Cambridge: Cambridge University Press, 2013.

[21] T. T. Nguyen, F. Laurent, R. O. Fox, and M. Massot, "Solution of population balance equations in applications with fine particles : Mathematical modeling and numerical schemes," *J. Comput. Phys.*, vol. 325, pp. 129–156, 2016.

[22] M. Pigou, J. Morchain, P. Fede, M. Penet, and G. Laronze, "New developments of the Extended Quadrature Method of Moments to solve Population Balance Equations," vol. 365, pp. 243–268, 2018.

[23] C. D. Pierce and P. Moin, "Progress-variable approach for large-eddy simulation of non-premixed turbulent combustion," vol. 504, no. March 2002, pp. 73–97, 2004.

[24] M. Ihme, C. M. Cha, and H. Pitsch, "Prediction of local extinction and re-ignition effects in non-premixed turbulent combustion using a flamelet/progress variable approach," *Proc. Combust. Inst.*, vol. 30, no. 1, pp. 793–800, Jan. 2005.

[25] N. Peters, "Laminar Flamelet Concepts in turbulent combustion," *Twenty-First Symp. Combust. Combust. Insititute*, pp. 1231–1250, 1986.

[26] G. Blanquart and H. Pitsch, "Chemical mechanism for high temperature combustion of engine relevant fuels with emphasis on soot precursors," *Combust. Flame*, vol. 156, no. 3, pp. 588–607, 2009.

[27] K. Narayanaswamy, G. Blanquart, and H. Pitsch, "A consistent chemical mechanism for oxidation of substituted aromatic species," *Combust. Flame*, vol. 157, no. 10, pp. 1879–1898, Oct. 2010.

[28] F. Nicoud, H. B. Toda, O. Cabrit, S. Bose, and J. Lee, "Using singular values to build a subgrid-scale model for large eddy simulations," *Phys. Fluids*, vol. 23, 2011.

[29] B. H. Toda, K. Truffin, B. Gilles, O. Cabrit, and F. Nicoud, "A dynamic procedure for advanced subgrid-scale models and wall-bounded flows," in *7th International Symposium on Turbulence and Shear Flow Phenomena, TSFP 2011*, 2011, vol. 2011-July, pp. 1–6.

[30] S. Popp, F. Hunger, S. Hartl, D. Messig, B. Coriton, J. H. Frank, F. Fuest, and C. Hasse, "{LES} flamelet-progress variable modeling and measurements of a turbulent partially-premixed dimethyl ether jet flame," *Combust. Flame*, vol. 162, no. 8, pp. 3016–3029, Aug. 2015.

[31] S. Gierth, F. Hunger, S. Popp, H. Wu, M. Ihme, and C. Hasse, "Assessment of differential diffusion effects in flamelet modeling of oxy-fuel flames," *Combust. Flame*, vol. 197, pp. 134–144, Nov. 2018.

[32] F. Hunger, M. F. Zulkifli, B. A. O. Williams, F. Beyrau, and C. Hasse, "Comparative flame structure investigation of normal and inverse turbulent non-premixed oxy-fuel flames using experimentally recorded and numerically predicted Rayleigh and OH-PLIF signals," *Proc. Combust. Inst.*, vol. 36, no. 2, pp. 1713–1720, 2017.

[33] P. Domingo, L. Vervisch, and D. Veynante, "Large-eddy simulation of a lifted methane jet flame in a vitiated coflow," *Combust. Flame*, vol. 152, no. 3, pp. 415–432, 2008.

[34] M. Ihme and H. Pitsch, "Prediction of extinction and reignition in nonpremixed turbulent flames using a flamelet/progress variable model. 2. Application in LES of Sandia flames D and E," *Combust. Flame*, vol. 155, pp. 90–107, 2008.

[35] P. A. Nooren, M. Versluis, T. H. Van Der Meer, R. S. Barlow, and J. H. Frank, "Raman-Rayleigh-LIF measurements of temperature and species concentrations in the Delft piloted turbulent jet diffusion flame," *Appl. Phys. B Lasers Opt.*, vol. 71, no. 1, pp. 95–111, 2000.

[36] P. P. J. Stroomer, "Turbulence and OH Structures in Flames," Technical University Delft, 1995.

[37] P. K. Sweby, "HIGH RESOLUTION SCHEMES USING FLUX LIMITERS FOR HYPERBOLIC CONSERVATION LAWS.," *SIAM J. Numer. Anal.*, 1984.

[38] P. Donde, V. Raman, M. E. Mueller, and H. Pitsch, "LES/PDF based modeling of soot–turbulence interactions in turbulent flames," *Proc. Combust. Inst.*, vol. 34, no. 1, pp. 1183–1192, Jan. 2013.

[39] F. Sewerin and S. Rigopoulos, "An LES-PBE-PDF approach for predicting the soot particle size distribution in turbulent flames," *Combust. Flame*, vol. 189, pp. 62–76, 2018.

[40] M. A. Schiener and R. P. Lindstedt, "Joint-scalar transported PDF modelling of soot in a turbulent non-premixed natural gas flame," *Combust. Theory Model.*, vol. 22, no. 6, pp. 1134–1175, 2018.